Relaxation in systems with exponential or Gaussian distributions of activation energies

J. Ross Macdonald
Department of Physics and Astronomy, University of North Carolina, Chapel Hill, North Carolina 27514

(Received 1 July 1986; accepted for publication 10 September 1986)

New expressions are presented, simplified, and discussed for the small-signal-frequency response of systems involving distributions of activation energies with either exponential or Gaussian probability densities. The results involve the possibility of separate but related thermal activation of energy-storage and energy-loss processes, and apply to the response of both dielectric and conductive systems. Response with a Gaussian distribution of activation energies (GDAE) may be either symmetric or asymmetric in log frequency, and typical GDAE responses are compared with those associated with several exponential distributions of activation-energy (EDAE) models, using complex nonlinear least-squares fitting. The GDAE model does not lead to the frequently observed fractional-exponent power-law response in time or frequency as does the EDAE; thus, the GDAE cannot fit any EDAE response well which involves an appreciable range of such behavior, but it is found that, conversely, the general EDAE model can often fit a GDAE response very well over a wide frequency range. Recent $(KBr)_{0.5}(KCN)_{0.5}$ dielectric data covering a range from $T = 13.7$ to 34.7 K are analyzed with the Cole–Cole, EDAE, and GDAE models, and the GDAE is found to yield the best overall fits. The results of the GDAE fits are analyzed in detail to illustrate the application of the GDAE model to real data. Contrary to the conclusions of an earlier analysis of the same data using an idealized, symmetric, and approximate GDAE model, we find that much of the data are better fit by a somewhat asymmetric, exact GDAE model which may involve a temperature-independent, finite-width Gaussian probability density. The present analysis suggests an alternative to the earlier results and suggestions that the width of the probability-density distribution increases with decreasing temperature and that the activation energies or barrier heights themselves depend linearly on temperature. The present data fit yield estimates of the lower limit of the temperature independent distribution of activation energies E_0 and of the more or less central activation energy E_1, but only set a lower limit for the value of the maximum activation energy of the distribution, E_∞. There is some evidence from the fitting that there may be a glasslike transition below about 4 K, but other effects outside the GDAE model may intervene before that temperature region is reached.

I. INTRODUCTION

The description of electrical (or mechanical) relaxation in a single crystal, liquid, or amorphous solid should ideally be based on the solution of an appropriate microscopic many-body model. Because of the complexity of such models with long range interactions, no accurate, analytic solution currently exists for any such real situation. Much of the earlier theoretical work in this area is listed in Ref. 1. There are currently virtually no accurate solutions of microscopic models which contain only microscopically defined parameters. The idealized models which have been treated usually involve one or more empirical parameters, ones without a detailed microscopic basis and either without specific temperature dependence or with such dependence only heuristically determined. A list of acronyms and major symbol definitions is included at the end of this paper.

Until realistic microscopic-model solutions become available, it is worthwhile to use semimacroscopic models. It has recently been shown[2–4] that such a model involving a double exponential distribution of activation energies (EDAE) can fit very well "data" derived from various earlier empirical relaxation expressions such as those of Cole and Cole,[5] Davidson and Cole,[6] Havriliak and Negami,[7] Williams and Watts,[8] and the "universal dielectric response" functions of Jonscher.[9] Thus the EDAE can, by extension, fit the vast number of small-signal frequency response data for dielectric and conductive systems which these expressions were originally used to fit. Unlike them, however, the EDAE model, which is based on a thermally activated response, predicts specific temperature dependence for its parameters, dependence of the form usually found experimentally.

In the meantime, however, several papers have recently appeared[10–13] which deal with relaxation or diffusion response by introducing a Gaussian distribution of activation energies (GDAE). An early discussion and use of the GDAE appeared[14] in 1942, but it has been introduced independently many times since then.

The GDAE assumption has the advantage that in some sense it is more "natural" than the EDAE, although the latter can be related to stochastic processes as well.[1,3,4] Although no detailed comparison between the frequency response predictions of the GDAE and EDAE models was available before the present work, it seemed likely at the beginning of this work that the EDAE could better fit more

 0021-8979/87/020700-14$02.40

temporal and frequency-response data than could the GDAE. In particular, the EDAE model always leads to response regions involving a (possibly fractional) exponent for t or $\omega \equiv 2\pi\nu$, e.g., t^{-n} and $\omega^{\pm m}$, where we take n and m as positive quantities. Such behavior is found to be virtually endemic in dielectric and conductive-system experimental data. But the GDAE model does not lead to response regions of finite length for which n or m are independent of t or ω. Nevertheless, as will be shown, the two models can yield a response which is quite similar in appearance if the response isn't extended very far into its tail regions.

Since the GDAE approaches used so far have been somewhat approximate, haven't systematically investigated the types of responses possible, and have not compared GDAE and EDAE responses, it seemed worthwhile to fill these gaps. A generalized GDAE model is presented and discussed, and both approaches will be used to analyze some $(KBr)_{0.5}(KCN)_{0.5}$ dielectric-response data.[10,15]

II. DERIVATION OF MODEL EQUATIONS

A. General response and activation-energy probability densities

By using properly defined and normalized quantities, it is possible to obtain both dielectric and conductive-system frequency responses from a single analysis.[3,4] The normalized dimensionless-response function for a single, possibly distributed dispersion region I_j, is defined as

$$I_j(\omega) = [U_j(\omega) - U_{j\infty}]/(U_{j0} - U_{j\infty}), \tag{1}$$

where $j = \epsilon$ or Z. Here U_{j0} and $U_{j\infty}$ are the $\omega \to 0$ and $\omega \to \infty$ limits of $U_j(\omega) \equiv U' + iU''$. When more than one dispersion region is present, clearly the $U_{j\infty}$ of the lowest frequency region must be the U_{j0} of the next dispersion region, and so on. With these definitions $U_\epsilon \equiv \epsilon = \epsilon' - i\epsilon'' \equiv \epsilon' + i\epsilon_n''$ and $U_Z = Z = Z' + iZ''$, an impedance. We shall derive expressions for I_j which apply for either dielectric or conductive systems and yield either the EDAE or GDAE response.

Assume that the relaxation process of interest is thermally activated but may possibly involve a more complex response than simple Arrhenius behavior. Any such process must involve both the storage and dissipation of energy. In the present quasimacroscopic approach we assume that $\mathscr{E} \equiv E/kT$ is distributed with a probability density $F(\mathscr{E})$, where E is an activation energy (enthalpy) for an elemental process such as dipole rotation, hopping of charges, etc. Now let us describe energy dissipation by means of a thermally activated elemental resistance R, and energy storage by a thermally activated elemental capacitor C.

We may write[3,4]

$$R_j = R_{aj} \exp(\alpha_j \mathscr{E}), \tag{2}$$

$$C_j = C_{aj} \exp(\beta_j \mathscr{E}), \tag{3}$$

and

$$\tau_j \equiv R_j C_j \equiv \tau_{aj} \exp(\gamma_j \mathscr{E}), \tag{4}$$

where R_{aj}, C_{aj}, and τ_{aj} are assumed temperature independent. The quantities α and β, however, may be temperature dependent, yielding nonArrhenius behavior.[1-4] In conventional treatments, α_j is usually taken as unity and β_j as zero; the present approach is more general, and β_j may even be negative for some processes. Finally, introduce a χ_j such that $\chi_\epsilon \equiv \beta_\epsilon$ and $\chi_Z \equiv \alpha_Z$.

We may now write an expression for the response function I_j for arbitrary $F(\mathscr{E})$. It is[3,4]

$$I_j(\omega) = \int_{-\infty}^{\infty} \frac{\exp(\chi_j \mathscr{E})\, F_j(\mathscr{E})\, d\mathscr{E}}{1 + i\omega\tau_j}, \tag{5}$$

where $\mathscr{E}$ is taken $\geqslant 0$ for physically realistic situations. From now on for simplicity the j subscript will be omitted with the understanding that the $I(\omega)$ results apply to either a dielectric or a conductive system. Normalization is assumed to be a part of $F(\mathscr{E})$ so that $I(0) = 1$, in agreement with Eq. (1).

In the general EDAE case, we may write

$$F(\mathscr{E}) = F_e(\mathscr{E}) = \begin{cases} 0, & \mathscr{E} < \mathscr{E}_0 \\ N\exp(-\lambda_1 \mathscr{E}), & \mathscr{E}_0 \leqslant \mathscr{E} \leqslant \mathscr{E}_1 \\ N\exp[(\lambda_2 - \lambda_1)\mathscr{E}_1 - \lambda_2 \mathscr{E}], & \mathscr{E}_1 \leqslant \mathscr{E} \leqslant \mathscr{E}_\infty \\ 0, & \mathscr{E} > \mathscr{E}_\infty, \end{cases} \tag{6}$$

where we have assumed $0 \leqslant \mathscr{E}_0 \leqslant \mathscr{E} \leqslant \mathscr{E}_\infty < \infty$, and N is a normalization factor. The minimum activation energy $\mathscr{E}_0$ may possibly be zero but the maximum value $\mathscr{E}_\infty$ must be finite for any real linear system, in agreement with the requirement that such a system has a longest relaxation time τ_∞ and a shortest relaxation time, τ_0. The quantity $E_1 \equiv kT\mathscr{E}_1$ implicit in Eq. (6) is a constant, possibly central, activation energy. In the above expression $\lambda_n \equiv \eta_n kT$, with $n = 1, 2$, and it is often reasonable to assume that the η_n's are temperature independent, thus making $F(\mathscr{E})/N$ independent of temperature. We then deal with a temperature-independent distribution of activation energies (TIDAE). Note that we may then write $\eta_n \equiv (kT_{Pn})^{-1}$ so that $\lambda_n = T/T_{Pn}$, where T_{Pn} is a constant temperature related to the strength of the exponential probability distributions.

For the GDAE situation we have

$$F(\mathscr{E}) = F_g(\mathscr{E}) = \begin{cases} 0, & \mathscr{E} < \mathscr{E}_0 \\ N\exp[-(\mathscr{E} - \mathscr{E}_1)/\delta]^2, & \mathscr{E}_0 \leqslant \mathscr{E} \leqslant \mathscr{E}_\infty \\ 0, & \mathscr{E} > \mathscr{E}_\infty. \end{cases} \tag{7}$$

This result follows from the standard form of the normal distribution[14] with variable E and parameters E_1 and σ. It follows that $\delta \equiv \sqrt{2}\sigma/kT$. Incidentally, the parameter σ of Ref. 10, say σ_B, is related to the present σ by $\sigma_B = \sqrt{2}\sigma$. Here the standard deviation σ is a width parameter; as $\sigma \to 0$, single time-constant Debye response is approached. Note that when $\mathscr{E}_0 = -\infty$ and $\mathscr{E}_\infty = \infty$, the normalization factor N is just the usual $(\sigma\sqrt{2\pi})^{-1}$. Certainly, we will never have $\mathscr{E}_0 < 0$ for any physical DAE case of interest, but when the range parameters $(E_1 - E_0)/\sigma$ and $(E_\infty - E_1)/\sigma$ exceed three, the above result for N will hold very accurately. Since these conditions will not always apply for the situations dis-

cussed below, we shall not use the above result for N but will handle normalization in another more general way to avoid possible loss of accuracy. If $F_g(\mathscr{E})/N$ is a temperature-independent probability density, σ must be temperature independent, and we may then define $T_P \equiv \sqrt{2}\sigma/k$; then $\delta = T_P/T$; compare the corresponding inverse parameters $\lambda_k = T/T_{Pk}$ of the EDAE.

B. EDAE-response models

Now in order to find a form of the EDAE $I_e(\omega)$ which involves a minimum number of separate parameters in the integral and to reduce the intercorrelation of parameters to a minimum, it proves convenient to introduce the new variable $x \equiv \gamma(\mathscr{E} - \mathscr{E}_1)$. Further, from Eq. (4) we may define the relaxation times $\tau_\infty \equiv \tau_a \exp(\gamma \mathscr{E}_\infty)$, $\tau_1 \equiv \tau_a \exp(\gamma \mathscr{E}_1)$, and $\tau_0 \equiv \tau_a \exp(\gamma \mathscr{E}_0)$. In previous work[3,4] we have defined the relaxation-time ratios $r \equiv r_2 \equiv \tau_\infty/\tau_0$, and $r_1 \equiv \tau_1/\tau_0$. Here we shall also deal with the natural logarithms of these quantities: $X_S \equiv \ln(r_2) = \gamma(\mathscr{E}_\infty - \mathscr{E}_0)$ and $X_L \equiv \ln(r_1) = \gamma(\mathscr{E}_1 - \mathscr{E}_0)$. The limits of $\mathscr{E}$ are $\mathscr{E}_0$ and $\mathscr{E}_\infty$; the corresponding x limits are $\gamma(\mathscr{E}_0 - \mathscr{E}_1) \equiv -X_L$ and $\gamma(\mathscr{E}_\infty - \mathscr{E}_1) \equiv X_U$. Notice that the relation $X_S = X_U + X_L$ follows from these definitions, as of course it must, since X_S is a measure of the full span of the $\mathscr{E}$ distributions. The τ in Eq. (5) may now be rewritten as $\tau_1 \exp(x)$. Finally, the normalized frequency variable is defined as $s \equiv \omega\tau_1$. In the earlier work the less appropriate choice $s \equiv \omega\tau_0$ was employed.

Using the above definitions, substituting Eq. (6) into Eq. (5), and selecting N so that $I(0) = 1$, one obtains

$$I_e(s) \equiv J_e(s)/J_e(0), \tag{8}$$

where

$$J_e(s) = \int_{-X_L}^{0} \frac{e^{\phi_1 x}\,dx}{1 + ise^x} + \int_0^{X_U} \frac{e^{\phi_2 x}\,dx}{1 + ise^x} \tag{9}$$

and

$$J_e(0) = \phi_1^{-1}[1 - \exp(-\phi_1 X_L)] + \phi_2^{-1}[\exp(\phi_2 X_U) - 1]. \tag{10}$$

In these equations

$$\phi_n \equiv \gamma^{-1}(\chi - \lambda_n), \quad n = 1,2, \tag{11}$$

in complete agreement with the earlier work.[3,4] Although Eqs. (8)–(10) may seem different from the equivalent equations given earlier,[4] they yield exactly the same numerical results and only differ in their parameterization. Note that when $\phi_2 > 0$, Eq. (9) is only convergent for $X_U < \infty$,[3] thus requiring $\mathscr{E}_\infty < \infty$.

For calculational purposes, it is better to rewrite Eq. (9) as

$$J_e(s) = \int_0^{X_L} \frac{e^{-\phi_1 x}\,dx}{1 + ise^{-x}} + \int_0^{X_U} \frac{e^{\phi_2 x}\,dx}{1 + ise^x}, \tag{9'}$$

with Eq. (10) remaining the same. Equations (8), (9'), and (10) define the most general form of EDAE response. It directly involves the five parameters ϕ_1, ϕ_2, τ_1, X_L, and X_U. If the system is thermally activated, τ_1 will show such activation and values of τ_1 will then lead to separate estimates of τ_a and $\gamma\mathscr{E}_1$. Note that although $X_L \equiv \gamma(\mathscr{E}_1 - \mathscr{E}_0)$ involves $\gamma\mathscr{E}_1$ as well, it is only equal to $\gamma\mathscr{E}_1$ if $\mathscr{E}_0 \equiv 0$.

In the general case, estimates of all the basic quantities E_0, E_1, E_∞, η_1, η_2, τ_a, α, and β cannot be directly obtained from data fitting at a single temperature. When data are available for a variety of temperatures, however, one can calculate estimates of the above eight basic parameters, especially when the forms of the temperature dependencies of ϕ_1 and ϕ_2 are known. Note that when $F_e(\mathscr{E})/N$ is temperature independent, as well as η_1 and η_2, the expected situation for many materials, then E_0, E_1, E_∞, and X_U/X_L will all be temperature independent. Further, comparison of the E_1 estimate obtained from τ_1 values with an $(E_1 - E_0)$ estimate obtained from X_L values will indicate whether E_0 is zero or not.

Although the general EDAE result above can fit a great deal of data,[3,4] there are two simplifications of it of interest. The first, the EDAE_1, generally gives asymmetric U'' vs $\log(s)$ and U'' vs U' curves, and applies when $F_e(\mathscr{E})$ involves only a single exponential. Then $\phi_1 = \phi_2 \equiv \phi$ and $X_L = X_U = X_S/2$. It follows that $\mathscr{E}_\infty - \mathscr{E}_0 = 2(\mathscr{E}_1 - \mathscr{E}_0)$ or, equivalently, $r_2 = r_1^2$. Then $\tau_\infty/\tau_1 = \tau_1/\tau_0 = \sqrt{r_2} = r_1$. Equations (9') and (10) reduce in this case for $\mathscr{E}_\infty < \infty$ to

$$J_e(s) = \int_0^{X_S} \frac{e^{-\phi x}\,dx}{1 + is_b e^{-x}}, \tag{12}$$

and

$$J_e(0) = [1 - \exp(-\phi X_S)]/\phi, \tag{13}$$

where $s_b \equiv s\exp(X_S/2) = \omega\tau_a \exp(\gamma\mathscr{E}_\infty) = \omega\tau_\infty$. Since $\mathscr{E}_1$ is not of importance in this case, it is not a parameter in (12) and (13) as it is in (9'). The EDAE_1 has the virtue that it involves two fewer free parameters than does the general EDAE but it is only appropriate for certain types of asymmetric data.

Another EDAE form, the EDAE_2, applies when data lead to symmetry in $\log(s)$ around $|U''_{\max}|$ [and thus in $U'(\omega)$ as well]. It also involves two less free parameters than the EDAE. In this case we may again take $X_L = X_U = X_S/2$ but let $\phi_1 = -\phi_2 \equiv \phi$. Then Eqs. (9') and (10) become

$$J_e(s) = \int_0^{X_S/2} e^{-\phi x}\left(\frac{1}{1 + ise^{-x}} + \frac{1}{1 + ise^x}\right)dx, \tag{14}$$

and

$$J_e(0) = 2[1 - \exp(-\phi X_S/2)]/\phi. \tag{15}$$

Here it turns out that when $\omega = \omega_p$, the frequency where $|U''(\omega)|$ is a maximum, then $s = s_p = 1$, so $\omega_p \tau_1 = 1$. In a symmetric case like this, one can thus obtain an estimate of τ_1 directly from ω_p without the need for detailed complex nonlinear least-squares (CNLS) data fitting.[16] It is worth noting that there is another simplification of the general EDAE which involves one more parameter than the EDAE_1 or EDAE_2 and leads to asymmetric response like, but not the same as, that of the EDAE_1 unless $X_U = 0$. For this model, the EDAE_3, we take $\phi_1 = -\phi_2$ as in the EDAE_2 but do not set $X_L = X_U$. As we shall see, taking different values of X_L and X_U can also lead to asymmetric response for the GDAE model, one commonly thought to yield completely symmetric response.

The condition $s_b = \omega\tau_\infty = 1$ in Eq. (12) does not yield a value of ω_p because of the ϕ-dependent asymmetry of the EDAE$_1$ curve.[3] For $\phi > 0$, the peak occurs at the low-frequency side of say a complex-plane plot of $-U''$ vs U', between $s_b = 1$ and $s_b = \sqrt{r_2}$, or, equivalently, between $\omega = \tau_\infty^{-1}$ and $\omega = \tau_1^{-1}$. Note that at the point $\omega = \tau_1^{-1}$, in the present case U' exactly equals $-U''$. For $\phi < 0$, on the other hand, it occurs between $s_b = 0.1$ and $s_b = 1$ for $r_2 \gg 1$. When ϕ is temperature dependent, it is thus inappropriate in the EDAE$_1$ case to examine ω_p for thermal activation since it depends on ϕ, τ_∞, and X_S. It is more sensible to obtain a τ_∞ estimate directly from CNLS data fitting at several temperatures of Eqs. (8), (12), and (13) and then test the results for thermal activation.

Equations (9'), (12), and (14) are all much preferable to the forms presented earlier.[3,4] For example, when exact "data" generated from the model, or such data truncated to three or four decimal places, are fitted by CNLS, the present forms generally yield better convergence, lower parameter intercorrelations, and smaller estimated relative errors of the parameters. Response curves for the EDAE, EDAE$_1$, and EDAE$_2$, have been presented earlier.[1-4]

C. The general GDAE-response model

A general expression for the GDAE $I_g(\omega) \equiv J_g(\omega)/J_g(0)$ response function is obtained when one substitutes Eq. (7) into Eq. (5). The result may be written

$$J_g(\omega) = \int_{\mathscr{E}_0}^{\mathscr{E}_\infty} \frac{\exp\{\chi\,\mathscr{E} - [(\mathscr{E} - \mathscr{E}_1)/\delta]^2\} d\mathscr{E}}{1 + i\omega\tau_a \exp(\gamma\,\mathscr{E})}, \quad (16)$$

with

$$J_g(0) = \int_{\mathscr{E}_0}^{\mathscr{E}_\infty} \exp\{\chi\,\mathscr{E} - [(\mathscr{E} - \mathscr{E}_1)/\delta]^2\} d\mathscr{E}. \quad (17)$$

In most earlier GDAE approaches no χ term appears, often an appropriate choice for dielectric systems but not for conductive ones, and it has been conventional to set $\mathscr{E}_0 = 0$ or even $-\infty$ and $\mathscr{E}_\infty = \infty$. Our present GDAE model obviously involves a truncated Gaussian distribution.

We have already pointed out that although the assumption $\mathscr{E}_\infty = \infty$ is not physically realistic, there are conditions where it and $\mathscr{E}_0 = 0$ lead to negligible loss of accuracy in (16). First, take $\chi \equiv 0$. Then if $(\mathscr{E}_1 - \mathscr{E}_0)/\delta$ and $(\mathscr{E}_\infty - \mathscr{E}_1)/\delta$ are both $\gtrsim 4$ or so, one may set $\mathscr{E}_\infty = \infty$ and $\mathscr{E}_0 = 0$ without appreciably affecting the value of $I_g(\omega)$. Under these conditions, (16) leads to a $-I_g''(\omega)$ result which is closely symmetric in ω around the $\omega = \omega_p$ point, where ω_p is the frequency at which $|I_g''(\omega)|$ is a maximum (peak frequency), namely $\omega_p \tau_1 = 1$. Further, Eq. (17) then accurately yields the conventional result $J_g(0) = \sqrt{\pi}\delta$. Since the symmetry conditions above are not always applicable, however, the GDAE can yield asymmetric curves as well as symmetric ones even when $\chi \equiv 0$.

When the transformation $x \equiv \gamma(\mathscr{E} - \mathscr{E}_1)$ is introduced into Eq. (16) and we take $s \equiv \omega\tau_1$ as before, one obtains

$$J_g(s) = \int_{-X_L}^{X_U} \frac{\exp[\theta x - (x/\xi)^2] dx}{1 + is e^x}, \quad (18)$$

where $\theta \equiv \chi/\gamma$ and $\xi \equiv \gamma\delta \equiv \gamma\sqrt{2}\sigma/kT$. Notice that unlike the EDAE situation, the θ and ξ (or ξ^{-1}) terms do not combine to yield a single ϕ parameter. Thus there are still five free parameters in Eq. (18) just as there are in (9'). It is easy to see from (18) that when $\theta \equiv 0$, $I_g''(s)$ will be completely symmetric in s around the $s = 1$ point provided $X_L = X_U \equiv X_S/2$. Such perfect symmetry is independent of the value of ξ, but only when $X_L = X_U \to \infty$ does one obtain exactly $J_g(0) = \sqrt{\pi}\,\xi$ from Eq. (18) with $s = 0$.

Let us define the response produced by Eq. (18) with arbitrary θ, X_U, and X_L values as general GDAE response. In analogy to the EDAE$_2$ situation, we may also define exactly symmetric GDAE$_2$ response as that obtained from (18) when $\theta \equiv 0$ and $X_U = X_L \equiv X_S/2$. The value of ω_p, where $-J_g''$, and $-I_g''$ are maximum, is again at $s = s_p = 1$, and thus $\omega_p = \tau_1^{-1}$ in this case.

Although experimental dielectric or conductive-system data often lead to symmetric response, it is also very common in both fields to find asymmetric response data, nearly always with the peak toward the low-frequency side [i.e., $-I_m''(\omega_p)$ occurs when $I'(\omega_p) > 0.5$]. Asymmetry arises whenever $X_U \neq X_L$ and/or when $\theta \neq 0$. Before discussing asymmetric behavior, to be identified as GDAE$_1$ response, it is useful to simplify the J_g (and I_g) expressions further. Even when $X_U = X_L$ but $\theta \neq 0$, it is found that not only is the response no longer symmetric but that $s_p \neq 1$. For appreciable θ and ξ values, s_p in fact differs very strongly from unity. It is thus desirable to introduce a new normalized frequency variable, for example, s_c, which will have a value s_{cp} at the peak of the $-I''$ vs s_c curve much nearer to unity than s_p when $\theta \neq 0$. Let us therefore define the new time constant $\tau_c \equiv \tau_1 e^A$, where the most appropriate choice of A will turn out to be $0.5\theta\xi^2$. Thus $\tau_c \neq \tau_1$ unless $\theta = 0$. It follows that $s_c \equiv \omega\tau_c = se^A$, so $s = s_c\, e^{-A}$. Then $J_g(s_c)$ may be written

$$J_g(s_c) = \int_{-X_L}^{X_U} \frac{\exp[\theta x - (x/\xi)^2] dx}{1 + is_c \exp(x - A)}. \quad (18')$$

Finally, set $y \equiv x - A$. It then surprisingly turns out that when $A \equiv 0.5\theta\xi^2$, as above,

$$I_g(s_c) \equiv J_g(s_c)/J_g(0), \quad (19)$$

where now

$$J_g(s_c) \equiv \int_{-(X_L + A)}^{X_U - A} \frac{\exp(-y/\xi)^2\, dy}{1 + is_c e^y}. \quad (20)$$

We see that the above transformations have allowed I_g to be expressed in conventional GDAE form (with possibly unequal limits) even when $\theta \neq 0$. Further, it is clear that only when $(X_U - A) = (X_L + A)$ will the response be fully symmetric.

Let us define new limit parameters of the integral as

$$X_{L\theta} \equiv X_L + A = \gamma(\mathscr{E}_1 - \mathscr{E}_0) + 0.5\theta\xi^2 \quad (21)$$

and

$$X_{U\theta} \equiv X_U - A = \gamma(\mathscr{E}_\infty - \mathscr{E}_1) - 0.5\theta\xi^2. \quad (22)$$

These expressions are very different from the conventional limit choices, 0 and ∞, and clearly contain important response information. It is now obvious that exactly symmetrical GDAE$_2$ response will occur in the most general ($\theta \neq 0$) case when $X_{L\theta} = X_{U\theta}$, or

$$\gamma(\mathscr{E}_\infty - \mathscr{E}_0) = 2[\gamma(\mathscr{E}_1 - \mathscr{E}_0) + 0.5\theta\xi^2]. \quad (23)$$

Note that $(X_{L\theta} + X_{U\theta})$ is still equal to X_S when $\theta \neq 0$ since θ does not affect the time-constant maximum ratio, $r_2 \equiv \tau_\infty/\tau_0$. In fitting data with Eqs. (19) and (20), there are now two possible approaches. First we may fit with only the four disposable free parameters, $X_{L\theta}$, $X_{U\theta}$, ξ, and τ_c. But these quantities do not allow θ, $\mathscr{E}_1$, $\mathscr{E}_\infty$, and τ_1 to be separately calculated. Thus, it is proper to use instead the free parameter set: X_L, X_U, ξ, τ_c, and θ. If the fitting results indicate that $\theta = 0$, it can then be eliminated as a separable variable in further fitting.

The temperature-dependence behavior of $X_{L\theta}$ and $X_{U\theta}$ is of special interest. Consider first the simplest case, that where δ, α, and β are temperature independent. Then

$$TX_{L\theta} = a + bT^{-1}, \quad (24)$$

$$TX_{U\theta} = c - bT^{-1}, \quad (25)$$

where a, b, and c are temperature-independent constants. When χ designates either α or β, their possible temperature dependence is of the form[3,4]

$$\chi = \chi_0[(T_0 - T)/T_0]\,[T/(T - T_\infty)], \quad (26)$$

where χ_0 is temperature independent, T_0 is a parameter specifying a possible linear relationship between activation enthalpy and activation entropy, and T_∞ is the Vogel–Fulcher temperature of a glasslike transition. When $T_0 \to \infty$ and $T_\infty \to 0$, $\chi \to \chi_0$. When T_0 and/or T_∞ play a role in the response, $TX_{L\theta}$ and $TX_{U\theta}$ will depend even more on T^{-1} than the simple dependence shown in Eqs. (24) and (25).

Finally, let us explicitly consider the conditions which allow the GDAE integral of Eq. (18′) to be closely approximated by the full Gaussian, Eq. (20) with $X_{L\theta}$ and $X_{U\theta}$ taken as infinite. Let us define the ratios

$$R_L \equiv X_{L\theta}/\xi = (\sqrt{2})^{-1}\{[(E_1 - E_0)/\sigma] + (kT)^{-1}\chi\sigma\} \quad (27)$$

and

$$R_U \equiv X_{U\theta}/\xi = (\sqrt{2})^{-1}\{[(E_\infty - E_1)/\sigma] - (kT)^{-1}\chi\sigma\}. \quad (28)$$

It turns out that $X_{L\theta}$ may be replaced by ∞ when $R_L \gtrsim 3$ or 4 and, as well, $X_{U\theta}$ replaced by ∞ when $R_U \gtrsim 3$ or 4. We may take the lower limit of discrimination (LLD) as $R_L = 3$. Thus when $X_{L\theta} \gtrsim 3\xi$, CNLS fitting with $X_{L\theta}$ a free parameter will be unable to yield a well defined estimate of $X_{L\theta}$. We may then set $X_{L\theta}$ to a fixed value for which $R_L > 3$ or 4. Larger values will not affect the accuracy of the fit and the estimates of the other parameters. The same considerations apply to the upper limit of discrimination (ULD) which we can set at $R_U = 3$. Again when $X_{U\theta}$ cannot be well determined from the data, it should be set to a large fixed value for which $R_U > 3$ or 4. It is clear from Eqs. (27) and (28) that the LLD and ULD will be temperature dependent when $\chi \neq 0$; the sign of χ determines which one increases and which one decreases as T increases. In the dielectric case where $\chi \equiv \beta$, when $\beta > 0$ (the usual situation) R_L will increase and R_U decrease as the temperature decreases. When $\chi = 0$ and $X_L = X_U = X_S/2 \equiv X_C$, as in the GDAE$_2$, the common limit of discrimination (CLD) is just $R_C \equiv X_C/\xi = 3$.

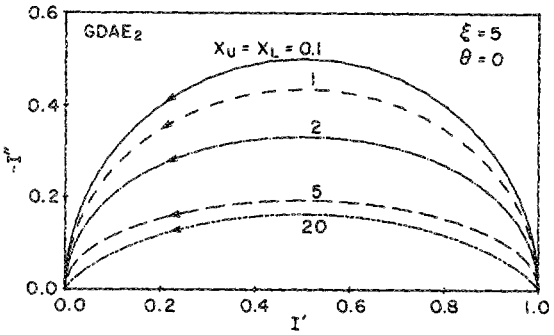

FIG. 1. Complex-plane plot showing symmetric GDAE$_2$ $I(\omega)$ response for $\theta = 0$, $\xi = 5$, and various $X_L = X_U$ values.

III. RESPONSE POSSIBILITIES AND GDAE-EDAE COMPARISONS

A. GDAE response

Although it is impractical to illustrate all the possible GDAE-response curve shapes, a few representative complex-plane results are presented in Figs. 1–4. Curves of $-I''$ vs $\log_{10}(s)$ will be presented later. The first two figures show various GDAE$_2$ symmetric response possibilities, while the last two illustrate two types of asymmetric, skewed responses. The results shown in these figures indicate that as $\xi \to 0$ and/or as X_L and $X_U \to 0$, single-time-constant Debye response is obtained. Note that the CLD is exceeded for several of the curves presented here.

Figure 4 shows typical $\theta \geqslant 0$ results; for negative θ values, left-skewed curves would result. Although the curves of both Figs. 3 and 4 are skewed, and both could be described by taking $\theta = 0$ and X_L and X_U as different values, the nonzero θ values of Fig. 4 result in simultaneous changes in both $X_{L\theta}$ and $X_{U\theta}$. Thus for $\theta = 0.5$, $X_{L\theta} = 16.25$, and $X_{U\theta} = 3.75$, while for $\theta = 1.8$, $X_{L\theta} = 32.5$, and $X_{U\theta} = -12.5$.

It has already been mentioned that the EDAE leads to power-law frequency response over a finite-frequency range while the GDAE does not. It is worthwhile to explore this difference. For the EDAE, let us define the power-law exponents n_r and n_i as being associated with $\omega^{\pm n}$ response for the

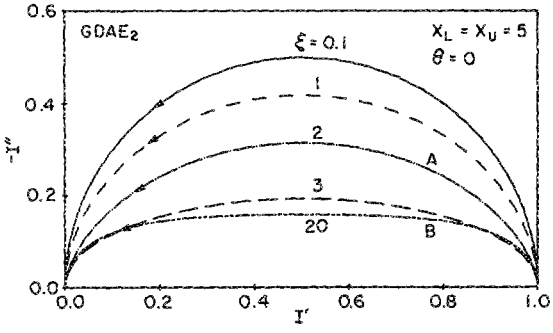

FIG. 2. Complex-plane plot showing GDAE$_2$ response for $\theta = 0$, $X_L = X_U = 5$, and various ξ values.

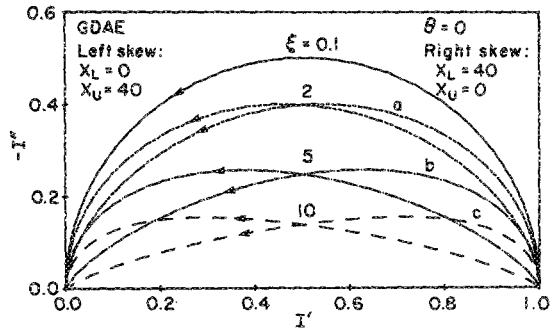

FIG. 3. Complex-plane plot showing asymmetric GDAE left- and right-skewed response for $\theta = 0$ and various ξ values.

real part I' and the imaginary part $-I''$ respectively. The plus sign applies for the $EDAE_1$, $EDAE_2$, and the general EDAE in the frequency region below that of the $-I''$ peak, and the minus sign for the $EDAE_2$ and general EDAE above this frequency, whenever $\omega^{\pm n}$ response regions appear.

Figure 5 shows typical results for the EDAE for two values of r_2. We see that n_r is not exactly the same as n_i, especially for the smaller r_2 curves. For $r_2 = 10^{12}$, however, the quantities are virtually the same in the range $0.2 \leqslant 0.8$ and are both close to ϕ. In this region of ϕ, the EDAE can yield, for large r_2, a response essentially the same as that of the constant-phase element (CPE) whose (nonrealizable) impedance over all frequencies may be written[4] as $Z = [A_1(i\omega)^n]^{-1}$. For large ϕ, $n_r \to 2$ and $n_i \to 1$, as required by the approach to single-time-constant Debye response as $\phi \to \infty$.[3,4]

The presence of $\omega^{\pm n}$ response leads to straight lines when the functions $S \equiv I^{-1}$ and $\log(S')$, and $\log(S'')$ are plotted in the complex plane.[3] Note that in the dielectric case the general function $S(\omega)$ becomes the complex modulus function, $M(\omega)$.[3] Figures 6 and 7 show such results for the $GDAE_2$ and for asymmetric GDAE situations. The low-frequency limit is at $S' = 1$ here. Figure 6 shows continuously curved lines; thus S' and S'' are not proportional to the same function of frequency. Figure 7 shows log results over a much wider range. At sufficiently high frequencies, S' reaches a constant value as required by physical realizability but even for $\xi = 5$, this value is not approached until $s \sim 10^{12}$. Only as ξ becomes quite large does the slope of the complex-plane line approach unity, necessary if, for example,

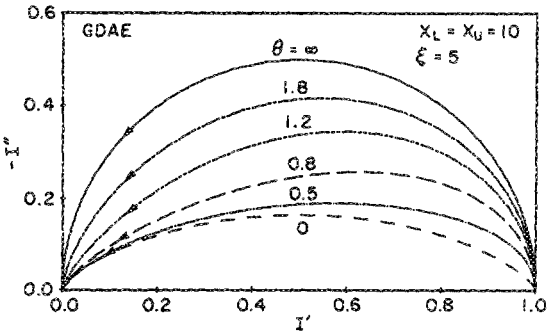

FIG. 4. Complex-plane plot showing GDAE response for $X_L = X_U = 10$, $\xi = 5$, and several θ values.

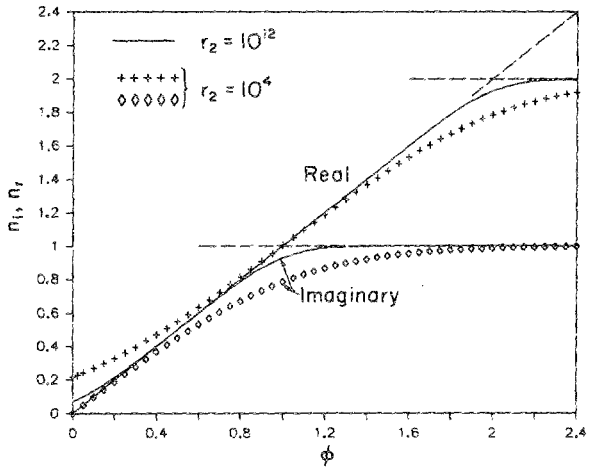

FIG. 5. The relations between EDAE fractional-power, frequency-response exponents, n_i and n_r, and the basic $EDAE_1$ or $EDAE_2$ parameter ϕ for two different r_2 values.

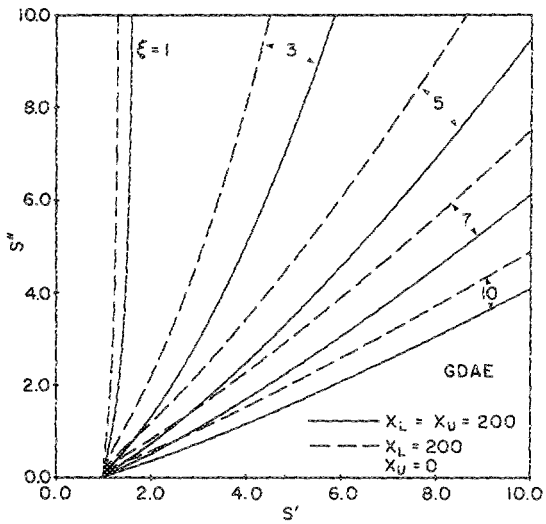

FIG. 6. Complex-plane plot showing GDAE $S(\omega) \equiv [I(\omega)]^{-1}$ response in the low-frequency region for different ξ values and symmetric and unsymmetric situations with $\theta = 0$.

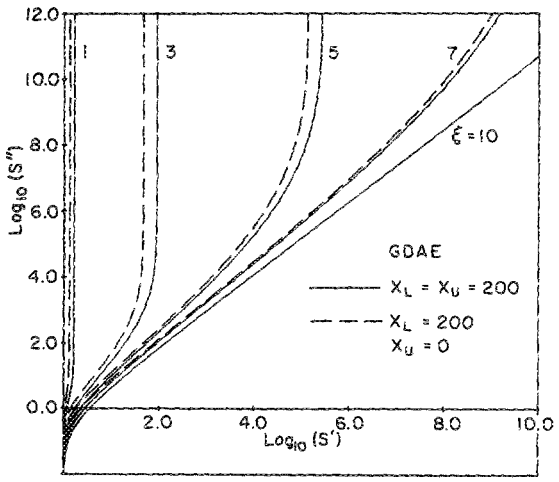

FIG. 7. Log-log complex-plane plot for the GDAE $S(\omega)$ function with $\theta = 0$ showing high frequency limiting behavior.

$S' \propto [f(\omega)]^{n_r}$ and $S'' \propto [f(\omega)]^{n_i}$, and $n_r = n_i$. The results of Figs. 6 and 7 should be compared with corresponding ones for the $EDAE_1$ in Ref. 3.

B. Width results

As we have seen, the quantity ϕ in the EDAE is closely related to the frequency-response power-law exponent. There is, however, no such analogous parameter in the GDAE model since it does not lead to such response. Instead, one may relate the standard-deviation parameter σ to the width of the $-I''(\omega)$ response curve in $\log(\omega/\omega_n)$ units. As customary, we shall take $\omega_n = 1\ \mathrm{s}^{-1}$ and suppress it hereafter.

Birge *et al.*,[10] in their fitting with an idealized GDAE dielectric model, have introduced a width, which we shall term w_e, defined as[17]

$$w_e \equiv \log_{10}(\omega_p/\omega_e), \tag{29}$$

where ω_e is that frequency above or below the peak frequency ω_p for which $\epsilon_e''/\epsilon_p'' = e^{-1}$. Here e is the base of natural logarithms. But as we have demonstrated, the GDAE need not yield symmetric response, and a half width such as that above is inappropriate for asymmetric response. Let us therefore define the general full width as

$$W_g \equiv \log_{10}(\omega_+/\omega_-), \tag{30}$$

where ω_+ and ω_- are the frequencies above and below ω_p at which $I''/I_p'' = q^{-1}$. If we again consider a symmetric situation and pick $q = e$, then $W_g \to W_e = 2w_e$. But it is more common to use $q = \sqrt{2}$ than $q = e$ for the definition of a width (half-power points). With this choice, let $W_g \to W$. We shall consider both W and W_e for the symmetric GDAE situation ($GDAE_2$) here.

What is the best way to estimate W or W_e from given data? Since real data are always contaminated with error, and usually only a relatively few $I''(\omega)$ data values are available, one should use all the data, where possible, to obtain a W estimate. If the data can be well fit to an appropriate model, such as the GDAE by nonlinear least squares or CNLS, then one can use the resulting best-fit parameter estimates to generate a large number of values of $I''(\omega)$ in the region $\omega < \omega_-$ to $\omega > \omega_+$ in order to determine $I''(\omega_p)$, ω_-, ω_+, $I''(\omega_-)$, and $I''(\omega_+)$ very accurately, thus using all the available data to obtain W_g. This approach is particularly useful for very wide $I''(\omega)$ curves such as those analyzed in Ref. 10.

The above procedure has been employed to calculate very accurate values of $W(\xi)$ and $W_e(\xi)$ for the present exact $GDAE_2$ model. Results are presented in Fig. 8. Note that as $\xi \to 0$, single-time-constant Debye response is approached; in this limit one readily finds that $W \cong 0.7656$ and $W_e \cong 1.4396$. The curves also show that the widths approach constant values as ξ increases for finite $X_L = X_S \equiv X_C$ values. Note that the large value $r_2 = 10^{24}$ corresponds to just $X_C \cong 27.6$. Only as $r_2 \to \infty$, not physically plausible, do the curves become completely straight lines in the large ξ region. In this limit one finds

$$W \to 0.511\xi \tag{31}$$

and

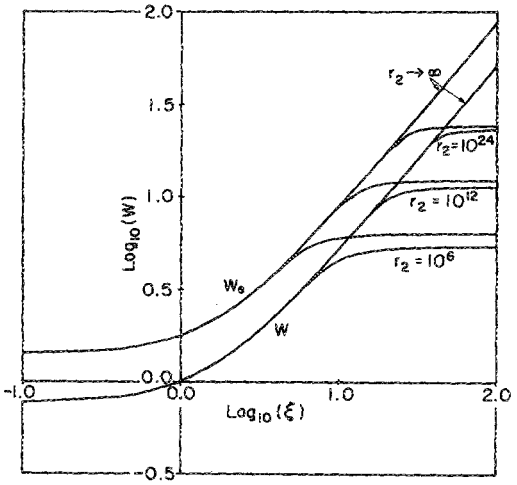

FIG. 8. Log-log dependencies of the two width measures, W_e and W, on ξ for various r_2 values.

$$W_e \to [2\log_{10}(e)]\xi. \tag{32}$$

It is also of interest to express these relations in terms of σ as well as ξ. One then finds

$$\sigma \cong 1.383(kT/\gamma)W, \tag{33}$$

and

$$\sigma = [\ln(10)/2\sqrt{2}](kT/\gamma)W_e \cong 0.8141(kT/\gamma)W_e. \tag{34}$$

Thus, given an estimate of W or W_e in the approximately straight-line region, one can estimate σ as well if γ is known. We may finally convert Eq. (34) to the Ref. 10 parameters σ_B and w_e and obtain

$$\sigma_B = [\ln(10)](kT/\gamma)w_e. \tag{35}$$

This result differs in two ways from that presented and used in Ref. 10: first, no γ is present there since the implicit assumption $\gamma = 1$ was made; in addition, the Boltzmann k factor is missing from the Ref. 10 expression.

C. GDAE and EDAE comparisons

Figures 9–12 show some comparisons of GDAE and EDAE responses. To carry out these comparisons many GDAE $I(\omega)$ values were accurately calculated and these "data" sets were fitted as well as possible by the EDAE model using CNLS. Two types of weighting were employed. In the P weight (PWT) situation, the uncertainties in I' and I'' values are taken proportional to the values themselves and the weighting for say a given I' value is calculated as $W_{I'} = s_{I'}^{-2}$, where $s_{I'}$ is the estimated uncertainty for an I' value. Conversely, for U weighting (UWT), the uncertainties are all taken as unity. Fitting with U weighting emphasizes the larger $-I''(\omega)$ regions at the expense of the smaller ones (tails) and yields smaller relative residuals in the large $-I''$ regions compared to those in the smaller I'' regions. Thus it yields a better fit for peak regions and a worse one for tails. On the other hand, P weighting tends to equalize relative residuals over the full data range. The PWT fitting results then appear worse on a linear plot and often better on a log plot. With negligible errors in the data and an

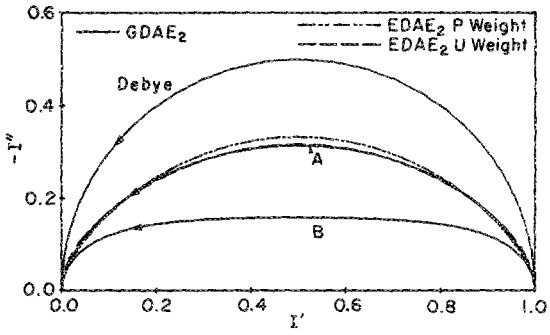

FIG. 9. Complex-plane plot showing comparisons of CNLS-EDAE$_2$ fits to GDAE$_2$ data of Fig. 2. P weight involves uncertainties proportional to data value magnitudes. U weight involves equal uncertainties.

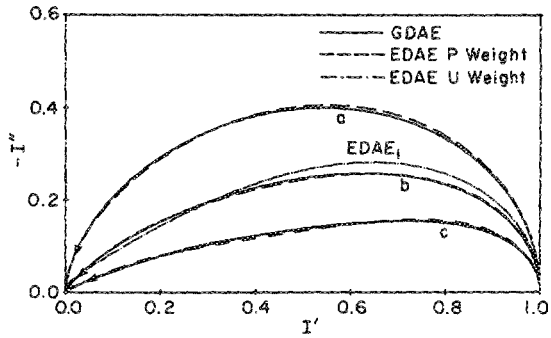

FIG. 11. Complex-plane plot showing comparisons of CNLS-EDAE and EDAE$_1$ fits to asymmetric GDAE data of Fig. 3.

appropriate fitting model, the two types of weighting will yield essentially the same parameter estimates. Fitting with these two types of weighting is illustrated in the next few figures.

Figure 9 is a complex plane presentation of the results of EDAE$_2$, CNLS fitting to the GDAE$_2$ curves marked A and B in Fig. 2. Perfect fitting of course occurs for the Debye curve, but we see that a nearly perfect PWT fit was obtained for the large-ξ B curve. As expected, U weighting gives a better appearing linear-plot fit for the smaller-ξ A curve than does the PWT choice. Figure 10 shows the same fitting results with $\log_{10}(-I'')$ plotted versus $\log_{10}(s)$, where here τ_1 was taken as unity. Although the UWT curve fits very well for the first decade or so of reduction of $-I''$ from its peak value, $-I''_p$, the fit is systematically worse for smaller I''/I''_p values. As shown, opposite behavior is found for P weighting. Even with either of these weightings for the curve A situation, quite accurate data would be required to allow one to discriminate adequately between GDAE and EDAE models here using CNLS fitting.

Figures 11 and 12 show EDAE fitting to the asymmetric GDAE curves marked a, b, and c in Fig. 3. We found that better fits were obtained with the general EDAE model than with the EDAE$_1$. A PWT EDAE$_1$ fit is included, however, for the b curve of both Figs. 11 and 12. No UWT fit is shown for this curve, but one sees that for all the general EDAE curves shown both PWT and UWT results are so close that one can not expect to be able to discriminate between the GDAE and EDAE models for any real data of this character extending over the present five decades of frequency.

Although the EDAE can fit the GDAE excellently here, we would not expect such good fits of the reverse situation: GDAE fitting to EDAE "data" which included $\omega^{\pm n}$ response over appreciable frequency ranges. Further, we find that the EDAE fit to the GDAE "data" does not yield EDAE parameter estimates well correlated with those used to calculate the GDAE points. For example, the curve-c GDAE-input parameter values were $\tau_1 = 1$ s, $\theta = 0$, $X_L = 40$, $X_U = 0$, and $\xi = 10$. Notice that $R_L = 4$ here, well above the LLD. Thus, even a GDAE fit to the very accurate GDAE synthetic data could do no more than establish that X_L was greater than 20 or so. The PWT CNLS EDAE parameter estimates and their estimated standard deviations were $\tau_1 = (5.9 \pm 0.7) \times 10^{-5}$ s, $X_L = 11.93 \pm 0.13$, $X_U = 9.60 \pm 0.11$, $\phi_1 = 0.2819 \pm 0.0024$, and $\phi_2 = 0.1064 \pm 0.0022$. U weighting yielded slightly different values with similar error estimates. Although the X_L and X_U estimates are quite different from the input ones, it is probably significant that $X_S = X_U + X_L$ is greater than 20 here for the EDAE fit.

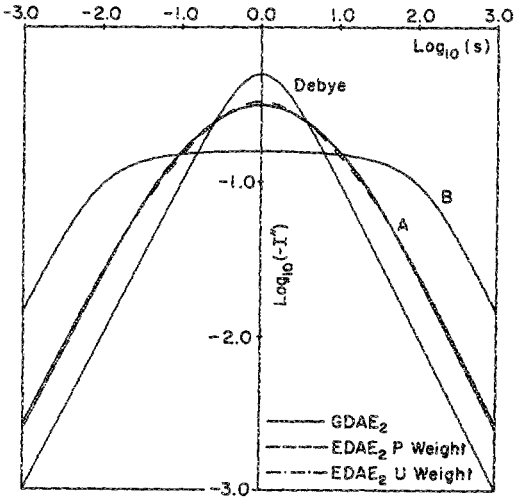

FIG. 10. Plots of $\log_{10}(-I'')$ vs $\log_{10}(s)$ for the various conditions of Fig. 9 showing the ability of the EDAE$_2$ model to fit GDAE$_2$ data.

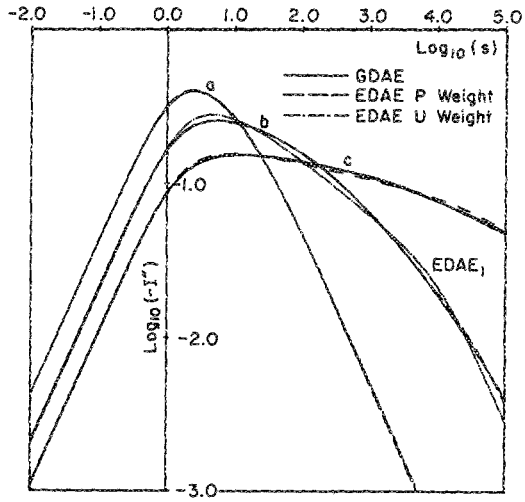

FIG. 12. Plots of $\log_{10}(-I'')$ vs $\log_{10}(s)$ for the various conditions of Fig. 11, again demonstrating the excellent fitting ability of the EDAE model.

The present results suggest that in many cases of interest the EDAE can well fit GDAE synthetic or real data, making discrimination difficult. But if the data include an appreciable region of fractional power-law frequency response, as most data do, we expect that the EDAE model will yield much the better fit.

IV. ANALYSIS OF $(KBr)_{0.5}(KCN)_{0.5}$ DATA

It is worthwhile to illustrate the use of the present generalized GDAE model by fitting some data likely to be appropriate for the model. Since the data of Birge *et al.*[10] on $(KBr)_{0.5}(KCN)_{0.5}$ has already been analyzed by these authors with an idealized GDAE, these data seemed especially suitable. It is of particular interest to investigate to what degree the new features of the present GDAE model allow more information to be derived from fits of real data than is possible with the idealized model. In particular, here we investigate the possible effects of $\mathscr{E}_0 \gtrsim 0$, $\mathscr{E}_\infty < \infty$, more exact normalization, and the influence of the possibly temperature dependent quantities α, β, and $\gamma \equiv \alpha + \beta$. Because we are dealing with dielectric system data here, $U_j(\omega) = U_\epsilon = \epsilon$, $I(\omega) = I_\epsilon(\omega)$, and $\theta = \chi_\epsilon/\gamma = \beta/\gamma$.

Unfortunately, only $\epsilon''(\omega)$ data for a wide variety of temperatures were available[15]; that for $\epsilon'(\omega)$ mentioned in Ref. 10 was not provided. Thus, CNLS fitting was precluded and only NLS fitting could be carried out using the relation $\epsilon''(\omega) = (\epsilon_0 - \epsilon_\infty) I''_\epsilon(\omega)$ which follows from Eqs. (1) and (5). We initially investigated the fits possible using the data sets for $T = 17.7$–34.7 K, the range over which $\epsilon''_p \equiv \epsilon''(\omega_p)$ fell within the measured frequency span.

Fits were carried out with the present GDAE, and, for comparison, with the EDAE, and the Cole–Cole DRT (CCDRT), whose $I(\omega)$ expression is[3–5]

$$I(\omega) = [1 + (is)^\psi]^{-1}. \tag{36}$$

This $I(\omega)$ leads only to symmetric response. Most of our fitting has been carried out with PWT, consistent with the assumption that the percent error in measured ϵ'' values is roughly constant. For many of the fits, parameter estimates were relatively insensitive to the choice of PWT or UWT.

Values of s_f, the standard deviation of the best overall fit, are shown in Table I for the temperatures and models considered. Both P and U weight results are given for $T = 34.7$ K because P weighting was unsatisfactory for this temperature. We see that for many of the temperatures there

TABLE I. Values of s_f, the standard deviation of the fit, for several models and temperatures.

		$s_f(\times 10^2)$		
T (K)	Weight	GDAE	EDAE	CCDRT
17.7	*P*	3.85	3.22	5.97
19.7	*P*	1.83	2.27	3.22
21.7	*P*	2.30	2.66	4.08
23.7	*P*	1.93	3.65	1.30
25.7	*P*	1.95	3.90	2.34
29.7	*P*	2.04	5.10	8.40
34.7	*P*	10.8	3.17	10.8
34.7	*U*	1.01	2.09	2.63

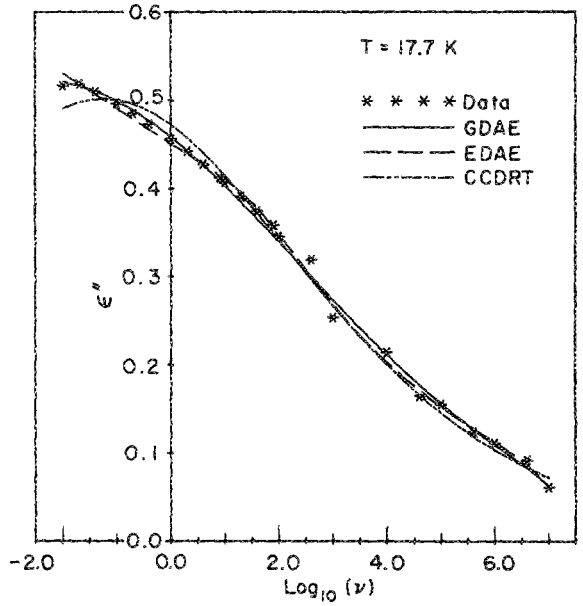

FIG. 13. Nonlinear least-squares fits, using various models with PWT, to the $(KBr)_{0.5}(KCN)_{0.5}$ dielectric data of Ref. 10 for $T = 17.7$ K.

is not a very large difference between the s_f's of the three models, although the GDAE does indeed seem preferable, across the board, to the other two models.

Figures 13–15 show results graphically for the two extreme temperatures and for one where ω_p falls near the center of the frequency span. Figure 15 illustrates the poor behavior of the GDAE- and EDAE-PWT fits for $T = 34.7$ K. A much better GDAE fit was obtained with U weighting, as shown. Its results are used in the following. It should be noted that the GDAE-UWT fit is not really very good in the low-frequency tail, however. For example, at $\nu = 10^{-2}$ Hz the data value of ϵ'' was 0.00912 while the fit prediction was 0.004 27.

Various trial fits of the $\epsilon''(\omega)$ data using the Eq. (20) GDAE model with θ a free parameter showed that it was

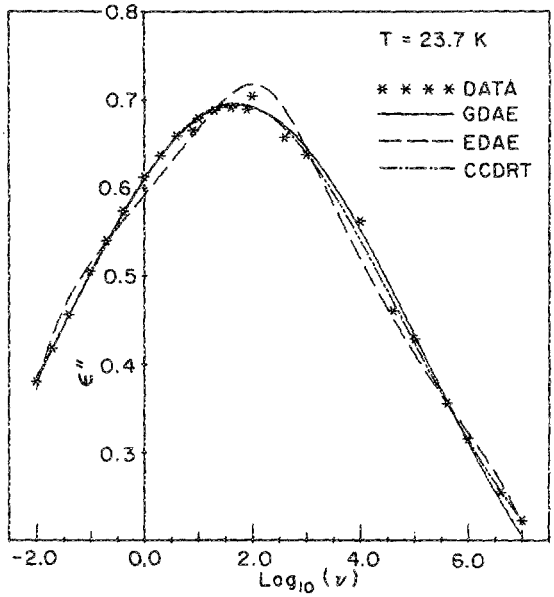

FIG. 14. Nonlinear least-squares fits, using various models with PWT, to the $(KBr)_{0.5}(KCN)_{0.5}$ dielectric data of Ref. 10 for $T = 23.7$ K.

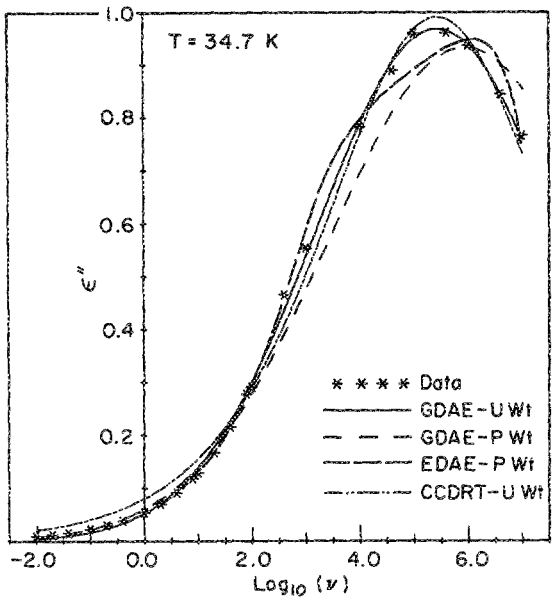

FIG. 15. Nonlinear least-squares fits, using various models with PWT and UWT, to the $(KBr)_{0.5}(KCN)_{0.5}$ dielectric data of Ref. 10 for $T = 34.7$ K.

impossible to determine any definite θ values. Similarly, no $X_{U\theta}$ values were well determined by the data; they were all above the UDL; thus $X_{U\theta} \gtrsim 40$ at $T = 17.7$ K and $X_{U\theta} \gtrsim 20$ at $T = 35.7$ K. We therefore used a constant value of $X_{U\theta} = 100$ at all temperatures. Note that the relatively large values of $X_{U\theta}$ implicit in the data by no means imply the appropriateness of the physically unrealistic values $X_{U\theta} = \infty$ and $\mathscr{E}_\infty = \infty$. For the present data the ϵ'' values have arbitrary units. Fitting yielded direct estimates of the scale factor $(\epsilon_0 - \epsilon_\infty)$ for each temperature. It was found that the final results were themselves quite well fitted by the empirical equation

$$(\epsilon_0 - \epsilon_\infty) = (6.84 \pm 0.13) + (40.0 \pm 3.1)T^{-1}, \quad (37)$$

with a s_f value of 0.07. Again the units of the quantity $(\epsilon_0 - \epsilon_\infty)$ are arbitrary.[10]

Although no well determined values of $X_{U\theta}$ were obtained from fitting with this quantity free, it was possible to obtain sensible $X_{L\theta}$ estimates for the lower five temperatures. The result that θ ($= \beta/\gamma$ here) was not directly determinable from the data suggested that $A = 0$ [Eq. (21)], and thus $X_{U\theta} = X_U$ and $X_{L\theta} = X_L$. The matter was resolved by noting that the fit values of $TX_{L\theta}$ did not show the T^{-1} behavior required by Eq. (24) when $\theta \neq 0$ and A is nonnegligible. Thus, we take $\beta = 0$ hereafter, as well as $X_{L\theta} = X_L$, $X_{U\theta} = X_U = 100$, and $\gamma = \alpha$. Although X_L should be within the LLD for all seven temperatures considered, judging from fits at the lower four or five temperatures, it did not turn out to be possible to obtain good estimates of X_L at $T = 29.7$ and 34.7 K, and the fixed value $X_L = 100$ was used for the final fits at these temperatures. Thus final fits using Eq. (18) involved the free parameters $(\epsilon_0 - \epsilon_\infty)$, τ_1, X_L, and ξ, or $(\epsilon_0 - \epsilon_\infty)$, τ_1, and ξ only.

Because of the large width of the $\epsilon''(\omega)$ data curves in $\log_{10}(\omega)$, Birge *et al.*[10] simplified the full GDAE expression by assuming that the Gaussian-width contribution dominated that from the Debye width. They thus took the latter contribution as a delta function of the form $\delta(\omega\tau - 1)$, leading[18] to the following approximate result:

$$\epsilon''(\omega) = (\pi/2)(w_e\sqrt{\pi})^{-1}[\log_{10}(e)](\epsilon_0 - \epsilon_\infty) \times \exp[-w_e^{-1}\log_{10}(\omega/\omega_p)]^2, \quad (38)$$

where w_e is related to σ_B by Eq. (35). Thus $\epsilon''(\omega)$ is forced to be symmetric in $\log_{10}(\omega/\omega_p)$.

Fitting with Eq. (38) was carried out[10] with NLS using[18] UWT, with the three free parameters $(\epsilon_0 - \epsilon_\infty)$, w_e, and ω_p ($= \tau_1^{-1}$). There is thus no possibility of obtaining an X_L estimate; full, symmetric Gaussian normalization was employed; and τ_1 equals $\tau_a \exp(E_1/kT)$ here since no γ parameter was introduced. These authors obtained generally good fits of the data, but their estimates of $(\epsilon_0 - \epsilon_\infty)$ are quite approximate, in part because the $\pi/2$ factor of Eq. (38) was not actually included in their work. In the present instance, where the units of ϵ are arbitrary, the matter is of little consequence. The needed $\pi/2$ factor is consistent with the Krönig–Kramers equations and, of course, with Eq. (38) fits of symmetric "data" calculated from the exact Gaussian-response function with $X_C/\xi > 4$. Further, while w_e is the exact half width for the approximate equation, it is only exact for the full GDAE model in the $\xi \to \infty$ limit. To avoid misinterpretation of w_e, it is better to replace the w_e's in Eq. (38) by $\xi \log_{10}(e)$, since ξ is the more fundamental quantity.

Equation (38) with w_e and $(\epsilon_0 - \epsilon_\infty)$ taken as free parameters gave very good PWT fits to exact symmetric "data" for $\xi = 21$, approximately the ξ value found for the $T = 13.7$ K data, the widest data set[10] considered here. The value of σ_f found was still reasonably good but was about 100 times larger for $\xi = 7$, near the $T = 34.7$ K data-set value found for this parameter. The fit value of ξ, calculated from estimated w_e values, was only about 0.6% too high at $\xi = 21$, increasing to about 5% too large, however, at $\xi = 7$. Thus, Eq. (38) is not a very close approximation for symmetric curves having ξ values corresponding to those found at the higher temperatures for the Birge *et al.*[10] data.

The present GDAE fits were found to be somewhat asymmetric at the lower temperatures. Let $J_g(0)$ be the value of the integral of Eq. (18) with θ equal to zero, $X_U = 100$, and X_L free. Let $J_{g\infty}(0)$ be the same quantity with $X_L = X_U \equiv X_C = 100$ or ∞. Its exact value is $\sqrt{\pi}\,\xi$. We found that the quantity $J_g(0)/J_{g\infty}(0)$ varied from 0.981 to 0.984 as the temperature went from 17.7 to 25.7 K. Thus ideal Gaussian normalization is a reasonably good, but not perfect, approximation for most of these data.

It is of interest to note that when the 17.7 K data were fitted with $X_L = 100$ fixed, rather than free, s_f turned out to be 4.68×10^{-2}, about 21% larger than that with X_L free. $\epsilon''(\omega)$ predictions with $X_L = 100$ fixed were of the order of 1–2% different for the low and mid frequencies, increasing to eight or nine percent in the high-frequency tail region. The estimates of the relative standard deviations of X_L obtained from the fitting at the different temperatures were as low as one percent but tended to increase with temperature.

Figure 16 shows results of the GDAE fits for ξ, X_L, and W_e points, with W_e values calculated by the method de-

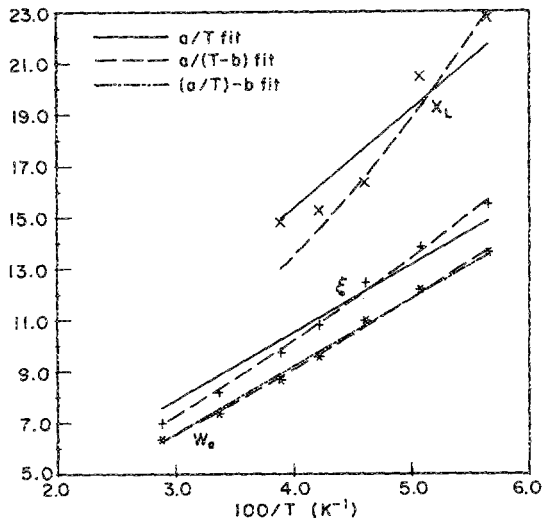

FIG. 16. Least-squares fits for the parameter estimates of the GDAE model for various functions of temperature.

scribed in the last section. Individual results are indicated with separate symbols; the lines show various LS fits to these derived values. With $\beta = 0$, the preceding definitions lead to

$$\xi = \alpha\sigma_B/kT, \tag{39}$$

$$X_L = \alpha(E_1 - E_0)/kT, \tag{40}$$

and

$$\tau_1 = \tau_a \exp(\alpha E_1/kT), \tag{41}$$

where α may have the temperature dependence given in Eq. (26). It is reasonable to take $\chi_0 \equiv \alpha_0 = 1$ here to set the scale of E. In trial fits of the ξ, X_L, and τ_1 values to the above formulas, we have been unable to obtain good results when both the T_0 and the T_∞ parameters of α were simultaneously free to vary; further, better results were obtained with T_∞ free than with T_0 free. Thus, we shall discuss further only possible α temperature dependence of the form

$$\alpha = (1 - T_\infty/T)^{-1}, \tag{42}$$

where T_∞ is related to a glasslike transition temperature.

We can initially eliminate the effect of any α temperature dependence by considering the ratio $\xi/X_L = \sigma_B/(E_1 - E_0) \equiv A_R$ which should be temperature independent for a temperature-independent DAE. Fitting with UWT yields $A_R = 0.693 \pm 0.010$, with a s_f of 0.66. Although the fit isn't perfect, it strongly suggests that ξ/X is indeed a constant for these data and that $(E_1 - E_0)$ and σ_B either have the same temperature dependence or, more likely, are temperature independent.

Parameter estimates and estimated standard deviations of the UWT fits shown in Fig. 16 are presented in Table II. Quantities without standard deviations given were taken fixed. In rows 1–3, $a \equiv \sigma_B/k$. All b values are for $b = T_\infty$ except those in rows 4 and 5 which are dimensionless. In these rows the empirical formula $W_{eB} = (a/T) - b$ employed by Birge *et al.*[10] was used. The results of row 4 are theirs; those of row 5 follow from the present GDAE fits. The remaining W_e fits of rows 6–8 use the more physically plausible expressions listed in Fig. 16. We see that the presence of a free or fixed (nonzero) T_∞ appreciably improves

TABLE II. Fitting results for the quantities plotted in Fig. 16.

No.	Quantity	a (K)	b	s_f
1	ξ	263.2 ± 4.9	···	0.56
2	ξ	212.2 ± 6.8	4.18 ± 0.55	0.20
3	ξ	222.1 ± 1.6	3.38	0.22
4	W_{eB}	262	-1.28	···
5	W_{eB}	270.1 ± 5.0	-1.65 ± 0.22	0.18
6	W_e	232.8 ± 2.6	···	0.40
7	W_e	195.6 ± 5.9	3.45 ± 0.53	0.17
8	W_e	196.4 ± 1.1	3.38	0.15
9	X_L	384.2 ± 10.4	···	1.10
10	X_L	293.1 ± 30.4	4.86 ± 1.57	0.87
11	X_L	321.0 ± 4.6	3.38	0.81

the fits, compared to the $T_\infty = 0$ choice, but the values of T_∞ found show appreciable scatter. We have, therefore, taken a weighted average of the T_∞ estimates determined from τ_1, ξ, and X_L fits, to obtain $\langle T_\infty \rangle = 3.38$ K. Results for this value, taken fixed, are also shown in Table II. We see that its presence usually decreases the estimated standard deviations of the parameter a or reduces s_f or both. If Eq. (32) held accurately over the present range of ξ, we would find $W_e \cong 0.8686\xi$. The results of rows 3 and 8 yield $W_e/\xi \cong 0.884$. Further, Fig. 16 shows that the ξ and W_e data points and lines (with b free) are not entirely parallel; thus, Eq. (32) is not completely applicable here, and ξ (or σ) is the more important parameter than W_e. It is clear that the X_L values are less accurate than those of ξ and W_e, and it is probable that the X_L estimate for $T = 25.7$ K, approaching the region where X_L could not be obtained from the data, is too large.

The determination of the best-fit parameters of τ_1, defined by Eqs. (41) and (42), is not entirely straightforward. One avoids introducing any bias by fitting directly to τ_1 with NLS rather than to $\ln(\tau_1)$ with ordinary LS. But what weighting is appropriate for such τ_1 fitting? If the estimated standard errors of the τ_1 values from the original GDAE fits involved no systematic errors, their use in determining the weighting (defined here as FWT) would be most appropriate. Another reasonable choice would be PWT. For fitting of $\ln(\tau_1)$ values, UWT is perhaps preferable to PWT if the range of $\ln(\tau_1)$ is not overly large. In the absence of other knowledge, one might pick that weighting which yielded the smallest estimates for the parameter standard deviations.

Fitting results for several of the above situations are presented in Table III. Here quantities Q and their estimated relative standard deviations s_{Qr} are shown in the form Q/s_{Qr}. For cross comparison we have included both τ_a estimates and $\ln(\tau_a)$ ones for both the τ_1 and $\ln(\tau_1)$ fits. Quantities without s_{Qr} values are calculated from the corresponding fit results. Birge *et al.*[10] found the following values from their fitting: $\tau_a \cong 3.125 \times 10^{-15}$ s, $\ln(\tau_a) \cong 33.4$, and $E_1/k \cong 659$ K. The results of rows 2 and 6 are quite comparable. Comparison of the results of rows 3 and 7, and 4 and 8 show that a nonzero free value of T_∞ slightly improves s_f values but yields larger s_{Qr} estimates here.

We may now use some of the foregoing results to calculate values of σ/k, $(E_1 - E_0)/k$, and finally E_1/k and E_0/k

TABLE III. Parameter estimates of τ_i with different types of fits and weighting.

No.	Quantity fitted	WT	$\ln(\tau_a)$	τ_a (s)	E_1/k (K)	T_∞ (K)	s_f
1	τ_i	F	-32.751	$5.98\times10^{-15}/0.18$	$640/7.6\times10^{-3}$	...	...
2	τ_i	P	-33.416	$3.07\times10^{-15}/0.26$	$659/9.2\times10^{-3}$	...	0.13
3	τ_i	P	-31.936	$1.35\times10^{-14}/0.56$	$589/4.2\times10^{-2}$	1.27/0.35	0.11
4	τ_i	P	-29.498	$1.55\times10^{-13}/0.26$	$481/1.1\times10^{-2}$	3.38	0.19
5	$\ln(\tau_i)$	P	$-33.764/7.5\times10^{-3}$	2.17×10^{-15}	$667/7.5\times10^{-3}$	...	...
6	$\ln(\tau_i)$	U	$-33.377/6.8\times10^{-3}$	3.20×10^{-15}	$659/8.0\times10^{-3}$	...	0.12
7	$\ln(\tau_i)$	U	$-31.992/3.3\times10^{-2}$	1.28×10^{-14}	$592/8.3\times10^{-2}$	1.21/0.75	0.11
8	$\ln(\tau_i)$	U	$-29.472/1.0\times10^{-2}$	1.59×10^{-13}	$481/1.2\times10^{-2}$	3.38	0.19

separately. For illustrative purposes we shall use fitting results where the fixed value $T_\infty = 3.38$ K was employed. We then find $\sigma/k \cong 157$ K, a temperature-independent quantity as it should be; $(E_1 - E_0)/k \cong 321$ K, also temperature independent; $E_1/k \cong 481$ K; and $E_0/k \approx 160$ K. The E_1 and E_0 estimates seem reasonable; they certainly would not be if it turned out that the data yielded $E_0 > E_1$. No E_0 estimate was possible for the Ref. 10 approach. Further, our results suggest that σ, the standard deviation of the DAE probability density, is temperature independent, contrary to the conclusions of Ref. 10. Although data fitting was unable to yield an estimate of E_∞/k, we may set a lower limit to this quantity by using Eq. (28) with $\beta = 0$ and taking $R_U = 3$. The estimates above then yield $E_\infty/k \gtrsim 802$ K. Alternatively, since the curves are reasonably close to being symmetrical, the condition $X_U = X_L$ may apply reasonably well. It leads for the above values, to $E_\infty/k \cong 1147$ K.

It is worth noting that Birge *et al.*[10] have discussed the possibility of barrier heights varying linearly with T, certainly not a temperature-independent DAE situation. Then the present E would be replaced by $E' \equiv E + \alpha_B T$. It was suggested that α_B was likely to be nonzero and positive, but it could not be obtained from their analysis. This transformation would only affect our expressions for X_L and X_U and would lead, for the present situation, to

$$X_L = (E_1 - \alpha_B T - E_0)/[k(T - T_\infty)], \qquad (43)$$

where E_1 and E_0 are now defined as the $T = 0$ values of these quantities. Because of scatter in the few X_L estimates available, we are unable to obtain sensible simultaneous estimates of $(E_1 - E_0)/k$, α_B/k, and T_∞. But with $T_\infty = 0$, fitting yields $(E_1 - E_0)/k \cong 491 \pm 66$ K and $\alpha_B/k \cong 5.1 \pm 3.1$ (thus virtually undefined), with an overall s_f of 0.93. Comparison of these results with those for rows 10 and 11 of Table II show that the choice $T_\infty \neq 0$, $\alpha_B = 0$ is appreciably better than the choice $T_\infty = 0$, $\alpha_B \neq 0$. Further, if α_B were non-negligible, the temperature independence of A_R discussed above would require that σ and σ_B would also have to be temperature dependent in the same way as X_L, a most unlikely situation. Nevertheless, the present result does not prove that $\alpha_B = 0$, only that this quantity is not determinable from the present data.

One test of consistency of some of the present results is to compare GDAE fit estimates for the $T = 13.7$ K data, not yet used, with estimates obtained from extrapolation of the present fit formulas for $(\epsilon_0 - \epsilon_\infty)$, τ_1, X_L, and ξ. We eliminated four outlying points from the $T = 13.7$ K data and found that appreciably smaller s_r values were obtained with UWT. Results are presented in Table IV. As usual X_U was taken as 100.

In Table IV the column 1 results were obtained with all the parameters free to vary. Note that τ_1 is very uncertain indeed here, primarily because the data did not include or extend close to $\epsilon''(\omega_p)$ so the peak frequency, τ_1^{-1}, is nearly undetermined. When τ_1 is fixed at its value extrapolated from the results in row 3 of Table III, one obtains the column 2 estimates. Finally, column 3 compares extrapolated estimates obtained entirely from the fits at higher temperatures with T_∞ free to vary. Although the column 2 s_f is larger than that for column 1, the column 2 results are much more consistent with those of column 3.

These results suggest, but do not prove, that it is indeed reasonable to use middle-range, fixed, extrapolated τ_1 values in GDAE fitting at temperatures outside that range where ω_p is included in the data. The present $\tau_1 \cong 5\times10^6$ s corresponds to a frequency whose period is about one year. It is thus impractical to make measurements which include ω_p on the present material at $T = 13.7$ K or below. One hopes that extrapolated results are still appropriate at these low temperatures, but as the temperature decreases one would expect tunneling effects to occur eventually and change the character of the response.

V. CONCLUSIONS

General forms for the EDAE and GDAE models have been presented and their use illustrated by fitting $(KBr)_{0.5}(KCN)_{0.5}$ small-signal response data by nonlinear least squares for an appreciable range of temperatures. A slightly asymmetrical general GDAE model proved to fit the data best. Analysis of the fit results strongly suggested that the activation parameter β of the model was zero, as well as any linear dependence on temperature of the activation ener-

TABLE IV. Comparison of three sets of parameter estimates for $T = 13.7$ K.

Quantity	1	2	3
$(\epsilon_0 - \epsilon_\infty)$	6.83 ± 0.30	10.50 ± 0.05	9.76
τ_1 (s)	$(1.36 \pm 0.76)\times10^4$	5×10^6	5×10^6
X_L	27.78 ± 0.52	33.10 ± 0.25	33.1
ξ	16.96 ± 0.39	20.58 ± 0.14	22.3
σ_f	3.3×10^{-3}	5.0×10^{-3}	...

gies themselves. The data led to estimates of the lower bound of the DAE, E_0, its approximately central activation energy E_1, and of the Gaussian probability-density width parameter σ. These quantities appear to be slightly temperature dependent if the activation parameter α is taken as unity (ordinary Arrhenius behavior). The DAE parameter E_0 was not obtainable from the earlier analysis,[10] but this work also led to some temperature dependence for E_1 and σ.

The temperature dependence of E_0, E_1, and σ very largely disappears when a glasslike transition is included in the model and thus α may be temperature dependent. The present introduction of physically plausible temperature dependence in a single parameter, which essentially eliminates that of E_0, E_1, and σ, thus leading to a TIDAE, seems preferable to accepting specific temperature dependence of these quantities for which no alternate plausible theory presently exists.

It should be finally emphasized, however, that there remains some possibility that the present generalized GDAE model is still not the most appropriate one for the present data and that the temperature dependence found of E_0, E_1, and σ, or of α, is just an indication of systematic errors arising from the choice of an inappropriate model. For the present data, which have fairly appreciable scatter, it is thus not yet possible to reach a completely firm conclusion that the activation-energy probability density of the material is temperature independent in the measurement range or not.

ACKNOWLEDGMENTS

I much appreciate helpful discussions with Dr. Norman Birge and Dr. Sidney Nagel, the valuable help of Larry D. Potter, Jr., and thank the U. S. Army Research Office for financial support.

LIST OF ACRONYMS AND MAJOR SYMBOLS

A. Acronyms

CCDRT:	Cole–Cole distribution of relaxation times.
CNLS:	Complex nonlinear least squares.
CPE:	Constant phase element.
DAE:	Distribution of activation energies.
EDAE:	Exponential DAE.
GDAE:	Gaussian DAE.
LLD:	Lower limit of discrimination.
LS:	Least squares.
PWT:	LS weighting using proportional uncertainties.
TIDAE:	Temperature-independent DAE.
ULD:	Upper limit of discrimination.
UWT:	LS weighting with equal uncertainties.

B. Major symbols

A number in parentheses indicates an equation where the symbol is used or defined.

k:	Boltzmann's constant.
m,n:	A power-law exponent in time or frequency.
n_i:	Power-law exponent for the imaginary part of model frequency response.
n_r:	Power-law exponent for the real part of model frequency response.
r,r_2:	$\tau_\infty/\tau_0 \equiv \exp[\gamma(\mathscr{E}_\infty - \mathscr{E}_0)]$.
r_1:	$\tau_1/\tau_0 \equiv \exp[\gamma(\mathscr{E}_1 - \mathscr{E}_0)]$.
s:	$\omega\tau_1$.
s_b:	$\omega\tau_\infty$.
s_c:	$\omega\tau_1 \exp(A)$.
s_f:	Estimated standard deviation of a LS fit.
s_p:	$\omega_p\ \tau_1$.
s_{Qr}:	Estimated relative standard deviation of quantity Q.
t:	Time.
w_e	Ref. 10 half width, (29).
x:	$\gamma(\mathscr{E} - \mathscr{E}_1)$.
A:	$0.5\theta\xi^2$, (21).
A_R:	$\xi/X_L = \sigma_B/(E_1 - E_0)$.
C_j:	Elemental thermally activated capacitance, (3).
C_{aj}:	Temperature independent limiting capacitance, (3).
$\mathscr{E}$:	E/kT.
E:	Activation energy (enthalpy); barrier height.
E_0:	Minimum activation energy of a DAE, (6).
E_1:	Activation energy appearing in τ_1.
E_∞	Maximum activation energy of a DAE, (6).
$F(\mathscr{E})$:	DAE probability density, (6), (7).
$I(\omega)$:	Normalized, general frequency response function, (1), (5).
$J(s)$:	Main response function of $I(s)$, (8).
$M(\omega)$:	Complex modulus function, $[\epsilon(\omega)]^{-1}$.
N:	Normalization parameter, (6), (7).
R_j:	Elemental thermally activated resistance, (2).
R_{aj}:	Temperature independent limiting resistance, (2).
R_C:	X_C/ξ, common value of R_L and R_U ($\theta = 0$).
R_L:	$X_{L\theta}/\xi$.
R_U:	$X_{U\theta}/\xi$.
$S(\omega)$:	$[I(\omega)]^{-1}$.
T:	Absolute temperature.
T_0:	(26).
T_∞:	Vogel–Fulcher temperature, (26), (42).
$U(\omega)$:	Frequency-response function, (1).
U_0:	$U(0)$.
U_∞:	$U(\infty)$.
W:	Full $I''(\omega)$ vs $\log_{10}(\omega)$ width, $q = \sqrt{2}$, (30).
W_e	Full $I''(\omega)$ vs $\log_{10}(\omega)$ width, $q = e$, (30).
X_C:	Common value of X_L and X_U.
X_L:	$\ln(r_1) = \gamma(\mathscr{E}_1 - \mathscr{E}_0)$.
$X_{L\theta}$:	(21).
X_U:	$\gamma(\mathscr{E}_\infty - \mathscr{E}_1)$.
$X_{U\theta}$:	(22).
X_S:	$\ln(r_2) = \gamma(\mathscr{E}_\infty - \mathscr{E}_0)$.
Z:	Impedance, $Z' + iZ''$.
α, α_j:	(2).
β, β_j:	(3).
γ, γ_j:	$\alpha + \beta$.
δ:	$\sqrt{2}\,\sigma/kT$, (7).

$\epsilon(\omega)$:	Complex dielectric constant, $\epsilon' - i\epsilon''$.
ϵ_p'':	$\epsilon''(\omega_p)$.
ϵ_0:	$\epsilon(0)$.
ϵ_∞:	$\epsilon(\infty)$.
η_n:	$n = 1,2$. λ_n/kT. Parameters in the EDAE probability density.
θ:	χ/γ, (18).
λ_n:	$n = 1,2$. $\eta_n\, kT$, (6).
ν:	Frequency, $\omega/2\pi$.
ξ:	$\gamma\delta = \sqrt{2}\,\gamma\sigma/kT$, (18).
σ:	$kT\xi/\sqrt{2}\,\gamma$. Standard deviation of Gaussian probability density.
σ_B:	$\sqrt{2}\,\sigma$.
τ_a, τ_{aj}:	Temperature independent limiting relaxation time (4).
τ_0:	Value of τ when $\mathscr{E} = \mathscr{E}_0$, $\tau_a \exp(\gamma \mathscr{E}_0)$.
τ_1:	Value of τ when $\mathscr{E} = \mathscr{E}_1$, $\tau_a \exp(\gamma \mathscr{E}_1)$.
τ_∞	Value of τ when $\mathscr{E} = \mathscr{E}_\infty$, $\tau_a \exp(\gamma \mathscr{E}_\infty)$.
ϕ:	Parameter in $EDAE_1$ and $EDAE_2$ models.
ϕ_n:	$n = 1, 2$, (11).
χ_j:	(5), $\chi_\epsilon \equiv \beta_\epsilon$, $\chi_Z \equiv \alpha_Z$.
ψ:	Exponent in CCDRT, (36).
ω:	$2\pi\nu$.
ω_p:	Angular frequency at which $\lvert I''(\omega)\rvert$ is a maximum.
ω_e:	Angular frequency where $\epsilon_e''/\epsilon_p'' = e^{-1}$, (29).

[1] J. R. Macdonald (unpublished).
[2] J. R. Macdonald, Bull. Am. Phys. Soc. **30**, 587 (1985).
[3] J. R. Macdonald, J. Appl. Phys. **58**, 1955 (1985).
[4] J. R. Macdonald, J. Appl. Phys. **58**, 1971 (1985). The following misprints should be corrected in this paper. In Eq. (17) the $\exp(-N_n E)$ term should be replaced by $\exp(-\eta_n E)$. In Eq. (24) the $\pm$ sign should be replaced by an equality sign.
[5] K. S. Cole and R. H. Cole, J. Chem. Phys. **9**, 341 (1941).
[6] D. W. Davidson and R. H. Cole, J. Chem. Phys. **19**, 1484 (1951).
[7] S. Havriliak and S. Negami, J. Polym. Sci. C **14**, 99 (1966).
[8] G. Williams and D. C. Watts, Trans. Faraday Soc. **66**, 80 (1970).
[9] A. K. Jonscher, Phys. Thin Films **11**, 202 (1980); see also *Dielectric Relaxation in Solids* (Chelsea Dielectrics, London, 1983).
[10] N. O. Birge, Y. H. Jeong, S. R. Nagel, S. Bhattacharya, and S. Susman, Phys. Rev. B **30**, 2306 (1984). The temperature given as 25.9 K in this work is properly 25.7 K.
[11] G. Carini, M. Cutroni, M. Federico, G. Galli, and G. Tripodo, Phys. Rev. B **30**, 7219 (1984).
[12] R. A. B. Devine, J. Appl. Phys. **58**, 716 (1985).
[13] B. Pistoulet, F. M. Roche, and S. Abdalla, Phys. Rev. B **30**, 5987 (1984). See also S. Abdalla and B. Pistoulet, J. Appl. Phys. **58**, 2646 (1985).
[14] W. Kaufmann, Rev. Mod. Phys. **14**, 12 (1942); see also J. R. Macdonald, J. Chem. Phys. **36**, 345 (1962).
[15] Data kindly provided by Dr. N. O. Birge.
[16] J. R. Macdonald, J. Schoonman, and A. P. Lehnen, J. Electroanal. Chem. **131**, 77 (1982).
[17] S. R. Nagel (private communication).
[18] N. O. Birge (private communication).